Dear Jennifer King and Paul Fleming,

We are pleased to submit for consideration our revised manuscript “Dynamic induction control for mitigation of wake-induced power losses: a wind tunnel study under different inflow conditions” (wes-2024-171).

We would like to sincerely thank the editorial team and the referees for their constructive feedback with valuable suggestions, which have significantly contributed to enhancing the quality and clarity of our paper.

All comments raised by the referees have been individually addressed in the detailed response below. The referees’ comments are listed in order of appearance in black font, followed by our corresponding **answers** or clarifications in green font, along with **actions** taken in the manuscript in blue font. Line, figure and table numbers in the referees’ comments are according to the initial manuscript. Language, spelling, style and other content refinements have been incorporated directly into the revised manuscript. All updated figures are included in the authors’ response.

We believe that the revised manuscript now meets the standards required for publication in Wind Energy Science journal. Please feel free to contact us if there are any remaining questions or if further clarification is needed.

Sincerely,

On behalf of all the authors,

Manuel Zúñiga

PhD Student

Referee 1

This paper describes an experimental study on dynamic induction control (DIC) to mitigate wind farm wake losses using physical models in a wind tunnel. The effect is found to be mostly dependent on inflow turbulence and the amplitude of the thrust oscillation. This study provides motivation for exploring DIC further for its application at full scale wind farms.

We sincerely thank the referee for their time and effort in thoroughly reviewing our manuscript. Below, we provide detailed responses to each comment and explain how we have addressed them in the revised manuscript.

Technical comments:

1. Please archive all code and data used to generate the results in a repository like Figshare or Zenodo and cite in the paper for the sake of reproducibility. This archive does not need to be cleaned up and fully-documented/user-friendly, but it should contain all files used in the study. Please also include the OpenFAST input/output files and plotting scripts used for the results shown in the appendix.

   An online database is currently being prepared including most relevant datasets and the corresponding DOI will be provided in the final publication.

2. **Line 171:** Is "Prandtl tube" intended to be "Pitot tube?"

   A Pitot tube only measures total (stagnation) pressure, whereas a Prandtl tube (also called Pitot-static tube) measures both total and static pressure. In our experimental setup, we used a Prandtl tube to determine the inflow wind speed from the dynamic pressure (i.e. pressure difference) using Bernoulli's principle. Hence, we have adhered to the term "Prandtl tube".

3. Is it possible to estimate pitch motor energy consumption to factor that into the overall energy gain?

   This could be an interesting analysis. However, we anticipate that the power gains achieved by downstream turbines would significantly outweigh the energy consumption associated with blade-pitch actuation, as DIC is designed for very low-frequency actuation within the partial load region. Moreover, this analysis falls outside the scope of our study, as the pitching mechanism of our model wind turbine is not scaled to account for factors such as pitch motor consumption, pitch inertia, and other potential losses. Such an assessment would require either numerical simulations or experiments with a full-scale turbine.

4. **Line 194:** Can you explain why the dataset became faulty?

   The raw WindScanner files were corrupted likely due to human error when loading the scanning trajectory for the corresponding downstream distance (*x/D* = 9). Unfortunately, this mistake was discovered after the wind tunnel campaign was over, and the data could not be postprocessed. Nevertheless, the uniformity of the inflow condition throughout the measurement domain has been verified (up to *x/D* = 16) in previous wind tunnel experiments (Hulsman et al., 2022b). Hence, it can be assumed that the uniform inflow condition in our experiments at *x/D* = 9 remained stable.

5. **Figure 5:** It would be valuable to know some indication of the uncertainty of these statistics.

To further elucidate the uncertainty in the measured wind fields, we have added a dedicated section to the appendix, as follows:

Appendix A: WindScanner measurement uncertainty

To illustrate the uncertainty in wake measurements obtained with the lidar WindScanner, Fig. A1a-c presents contours of the relative error (e_u/u) introduced by the single-Doppler reconstruction of *u* at downstream distances x/D ∈ {2, 5, 9}, while Fig. A1d-f shows the corresponding statistical uncertainty at the same locations. The displayed contours correspond to experiments under uniform inflow with WT1 actuation at *St* = 0.30 and *A* = 2°. The analysis of e_u/u follows the standard uncertainty propagation method (JCGM, 2008; van Dooren et al., 2017; Hulsman et al., 2022b), expressed as:

$$e_u = \sqrt{\left(\frac{\partial u}{\partial v_{\mathrm{los}}}\delta_{v_{\mathrm{los}}}\right)^2 + \left(\frac{\partial u}{\partial v}\delta_v\right)^2 + \left(\frac{\partial u}{\partial w}\delta_w\right)^2 + \left(\frac{\partial u}{\partial \phi}\delta_\phi\right)^2 + \left(\frac{\partial u}{\partial \theta}\delta_\theta\right)^2}$$

where $\delta_{v_{\mathrm{los}}}$ is the uncertainty of the measured line-of-sight wind speed, assumed to be 1% of u_∞. δ_v and δ_w represent the uncertainties arising from neglecting the *v* and *w* components, conservatively assumed as 1 ms^{-1}. δ_ϕ and δ_θ refer to the uncertainties in the azimuth and elevation angles, each assumed to be 0.5 mrad. Additionally, the statistical uncertainty is expressed in terms of the margin of error $e_{\mathrm{MOE}} = z_\gamma\, \sigma/\sqrt{N}$, where z_γ = 1.96 is the quantile corresponding to a 95 % confidence interval, σ is the standard deviation of the measurements and *N* is the sample size.

In general, e_u/u is higher within the wake and closer to the rotor, since the wind speed deficit is more pronounced. Similarly, a higher e_{MOE} is observed in regions of higher turbulence due to increased fluctuations within the wake.

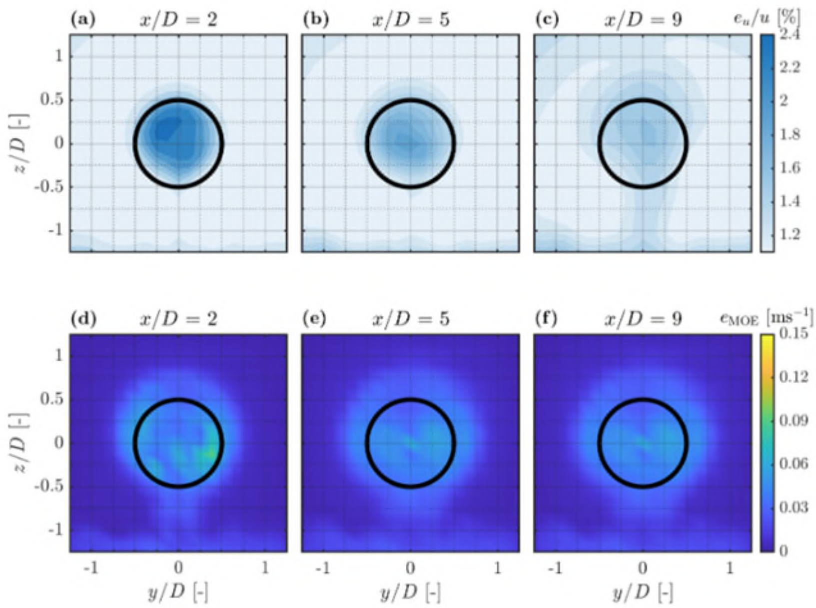

Figure A1. Uncertainty in the streamwise velocity component measured with the WindScanner at downstream distances x/D ∈ {2, 5, 9}. The top row (a-c) shows the relative error (e_u/u) introduced by the single-Doppler reconstruction, while the bottom row (d-f) presents the statistical margin of error (e_{MOE}). All wake contours correspond experiments under uniform inflow with upstream turbine actuation at St = 0.30 and A = 2°.

6. What is the mechanism by which wake recovery is enhanced with DIC, i.e., is there a difference in the mean flow structure or is this all turbulent transport? The paper mentions vortex rings, which are certainly different from isotropic homogeneous turbulence. Do these vortex rings have any significance, or is it simply a means to inject energy that breaks down into something like isotropic turbulence to increase transport?

   To give further insights, we have extended the analysis of turbulence development in the wake of WT1 in Sect. 3.1.2, focusing on the downstream evolution of local power spectra at the wake centre. Specifically, the following text has been added:

   As a second metric, Fig. 8 compares the downstream evolution of the local power spectra $\phi_{u'}$ along the wake centreline *y/D* = 0 for the greedy case and two DIC cases with the same *St* = 0.30 but different amplitude. This provides insight into the wake energy distribution across different turbulence scales, as well as the presence of coherent structures. The power spectra are computed with the standard Welch's algorithm in MATLAB (2024), using the local time series of the wind speed fluctuations, $u'(y) = u(y) - \langle u(y) \rangle$. The frequency axis is expressed in terms of the dimensionless Strouhal number. In general, the energy content remains largely unchanged across all downstream locations for the baseline greedy case, consistent with the slow turbulence build up observed in the local TI profiles. On the other hand, the DIC cases exhibit not only higher energy spectra but also distinct peaks at the frequency of pitch actuation *St* = 0.30 and its higher harmonics. This indicates the presence of large-scale coherent structures, which can be associated with the emergence of vortex rings, as reported in (Munters and Meyers 2018; Yılmaz and Meyers 2018). In fact, Yılmaz and Meyers (2018) show that these structures cause an earlier wake breakdown, enhancing the momentum entrainment into the wake core. Furthermore, comparing the spectra of different amplitude cases, the convergence to a single spectrum with similar energy across all frequencies by *x/D* = 3 indicates an earlier transition to the far-wake region for the high amplitude case (A = 2°). The zoomed-in view of the dominant peak at *St* = 0.30 confirms that a turbulence plateau is reached at *x/D* = 3, followed by a decay at x/D = 5. In contrast, the low-amplitude case (A = 1°) exhibits a slower turbulence build-up, with the highest energy content observed at *x/D* = 5. Additionally, although not shown here, spectral analysis of the shear layer region at the rotor edges reveals an even more rapid turbulence development for both amplitude cases. This is reasonable since the transition to the far-wake region starts with the breakdown of the helical tip-vortex system into small-scale turbulence structures (Lignarolo et al. 2015) but also results in the formation of vortex rings due to periodic flow disturbances induced by DIC. This fuels momentum transport towards the wake core in response to a faster shear layer expansion.

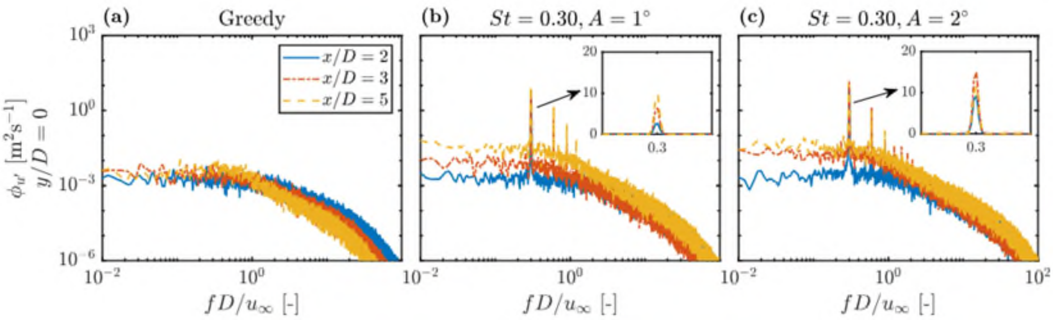

Figure 8. Downstream evolution of the local power spectra of wind speed fluctuations ($\phi_{u'}$) at the wake centreline (y/D = 0) of WT1 under uniform inflow conditions. For DIC cases, zoomed insets illustrate the downstream development of the dominant coherent structure at St = 0.30.

7. What is the difference between the Reynolds number of this study and a full-scale wind turbine, and how might that affect the conclusions?

The Reynolds number (*Re*) mismatch between model wind turbines and full-scale turbines is a well-known drawback when performing wind tunnel experiments. Nonetheless, several studies (e.g. Vermeer et al., 2003, Chamorro et al., 2012, Wang et al., 2021) indicate that the main wake features (e.g. wake deficit, turbulence intensity, shear stresses) can be reproduced once a minimum Re is achieved. In particular, Chamorro et al., (2012) suggest *Re* independence for rotor-based *Re* > 9.3×10^4. Since all our experiments were conducted at around *Re* = 2.9×10^5, it is assumed that the wake generated by the model wind turbine resembles well that of full-scale turbines.

To further clarify the implication in *Re* mismatch between model wind turbines and full-scale turbines, we have added the following text to the methodology under the "Model wind turbine" subsection:

To account for scaling effects and manufacturing constraints, the blades feature an SD7003 low-Reynolds-number (*Re*) airfoil with increased chord length and tailored twist distribution along the span (Schottler et al., 2016). While this improves aerodynamic performance in the operating low-*Re* regimes typical of wind tunnel testing, the power coefficient (C_P) remains unavoidably lower than that of full-scale turbines (Wang et al., 2021).

As well as the following text to the methodology under the "Experimental setup and measurement procedure" subsection:

All experiments were conducted in the partial load region at u_∞ = (7.0 ± 0.1) ms^{-1}, resulting in a rotor-based Reynolds number of *Re* ≈ 2.9×10^5. Although lower than that of full-scale turbines, typically $\mathcal{O}(10^6)$ to $\mathcal{O}(10^7)$, Chamorro et al., (2012) suggest *Re* independence of the main wake statistics for rotor-based *Re* > 9.3×10^4.

8. **Line 273:** What type of low pass filter was applied?

To clarify, we have added the following sentence:

...the raw signals are low-pass filtered at 12 Hz to remove high-frequency noise and facilitate visualisation. To eliminate phase distortion, a sixth-order Butterworth filter is applied using the filtfilt function in MATLAB (2024).

Furthermore, the values in Table 2 and Table 3 have been updated using a cut-off frequency of 250 Hz (i.e. about 12P of the once-per-revolution (1P) cyclic load). This choice filters out high-frequency noise while preserving most relevant dynamic components. Further increases in the cut-off frequency resulted in negligible variations.

We have added the following sentence:

.. The reported values represent 10-min averages, obtained after low-pass filtering the data at 250 Hz. This choice filters out high-frequency noise while preserving most relevant dynamic components. Further increases in the cut-off frequency resulted in negligible variations.

9. **Line 323:** The wording is confusing here. Since WT3 does not actually exist, how can it be operating in greedy mode?

   This is an assumption based on the use of WT1's optimal C_P under greedy mode to calculate the virtual turbine power of WT3.

   To clarify, we have reformulated the text as follows:

   WT3's virtual power is estimated from the u_{REWS} computed in Sect. 3.2.1 assuming greedy operation with the same optimal efficiency as WT1 (C_P = 0.37), without accounting for *Re* effects. Accordingly, only WT1 alternates between greedy and DIC modes, while WT2 and WT3 remain in greedy mode throughout.

10. Would it be possible to optimize tip speed ratio concurrently with pitch-actuated thrust oscillation to minimize power loss at the upstream turbine?

    The baseline generator torque controller was kept active during all DIC mode experiments. This controller tries to maintain operation at the point of optimal aerodynamic efficiency (C_P^*), which corresponds to the turbine's optimal tip speed ratio under steady-state conditions, as already detailed in section 2.3, L. 117.

    However, it is worth noting that due to pitching around fine pitch angle, the average C_P value is slightly reduced, which is not accounted for in the standard $K\omega^2$ torque control. Whether this could lead to a higher power gain is beyond the scope of this paper, as further experiments would be needed to test and validate this hypothesis.

    The following text has been added to methodology under the DIC mode section:

    Although pitch actuation causes fluctuations and a reduced mean in $\mathrm{C_Q}$, the controller gain *K* is not updated during the experiments.

11. How are the turbines' power losses measured? Similarly, are the downstream turbine's power gains measured with REWS or from an electrical power measurement?

    The power losses due to DIC activation are calculated relative to the measured power of WT1 in greedy mode for each inflow type. For WT2, power gains are determined similarly using measured power. Only WT3 is estimated based on the power of a virtual turbine, derived from the rotor-equivalent wind speed.

    We have reformulated the text in Sect. 3.3 as follows:

    Figure 14 displays the mean power ratio ($P_\mathrm{i}/P_\mathrm{ref}$) for individual turbines (WT1, WT2, WT3) and the entire wind farm (WF), where P_i represents a 10-min average of the measured electrical power at WT1 and WT2, and the virtual power of WT3. $P_\mathrm{ref} = \sum_{i=1}^{3} P_{i,\mathrm{Greedy}}$ is the total wind farm power output when all three turbines operate in greedy mode. Each subchart corresponds to a different inflow condition, with percentage values indicating the relative change for individual turbines and the whole wind farm with respect to the baseline greedy case.

    Note that as suggested by Referee 2, we have also added a comparison of real-virtual-virtual turbine configuration to the appendix in the revised manuscript (cf. response to Referee 2 below), where both WT2 and WT3 are based on virtual power estimates.

12. **Line 362:** Is it true that there was improved wake recovery but no improvement in waked turbine power?

    The improvement in wake recovery is demonstrated in Figs. 5, 6, 9 and 10 based on WindScanner measurements, while the increase in power is shown in Fig. 12, derived from WT2's electrical power measurements and WT3's virtual power across all DIC cases and inflow conditions. The absence of net power gains at the farm level under ABL Type-II is primarily due to the higher power losses experienced by the model wind turbine compared to those expected in full-scale turbines (cf. Appendix B in the original manuscript), as well as the reduced power gains in downstream turbines (WT2 and WT3) due to increased inflow turbulence.

    For better clarity, we have added the following lines in the discussion:

    ...although control authority is notably reduced under ABL Type-II inflow, this study underscores the potential adaptability of DIC to realistic inflow conditions.

    ...the assessment of wind farm power gains in a virtual three-turbine configuration demonstrates consistent power benefits under uniform and ABL Type-I inflows. The absence of net power gains at the farm level under ABL Type-II is primarily due to the higher power losses experienced by the model wind turbine (approximately 10 %) compared to those expected in full-scale turbines. Supporting this, aerolastic simulations using the NREL–5 MW reference turbine (D = 126 m) show power losses below 1.6 % for all DIC cases under both uniform and ABL inflows (cf. Appendix D). These results are more closely aligned with reported losses from LES studies using actuator disc or actuator line models (e.g. Yılmaz and Meyers, 2018; Frederik et al., 2020a; Coquelet et al., 2022).

13. **Line 407:** What about main bearing loading?

    The cited paper does not address the assessment of main shaft bearing loading, only pitch bearing load. Further studies are required to evaluate the impact on other load components.

14. **Figure 12:** Is it possible to put error bars here?

    The Figure below includes error bars in grey. For the values based on the electrical power of physical turbines ($WT1_{Real}$ and $WT2_{Real}$), the statistical margin of error was used. For the virtual turbine ($WT3_{Virt}$) and the wind farm power (WF), standard error propagation was applied. Since the error bars are nearly imperceptible due long measurements with high sampling frequency, we decided to exclude them, consistent with the initial manuscript.

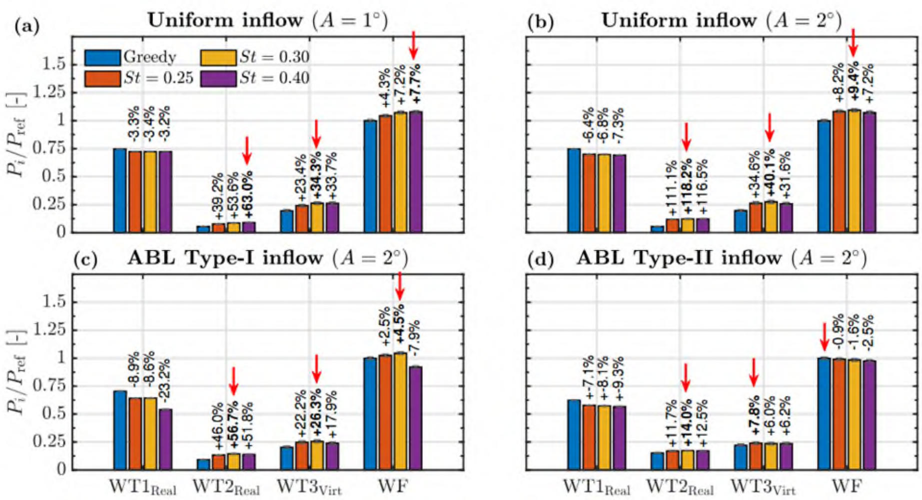

Figure AR01. Illustration of wind farm power gains, including error bars (Fig. 12 in the original manuscript)

15. **Figure 12:** Why are losses so high with St = 0.4 in ABL type-I inflow (subplot c)? Is there any evidence that this is attributable to vibration or resonance as hypothesized? Is it possibly a measurement error?

We have further analysed the data and found that the high-power loss was caused by large fluctuation in generator torque, which in turn led to significant power fluctuations. This is evidenced by the higher energy content in the power spectrum for the St = 0.40 case compared to the other cases (see Figure below).

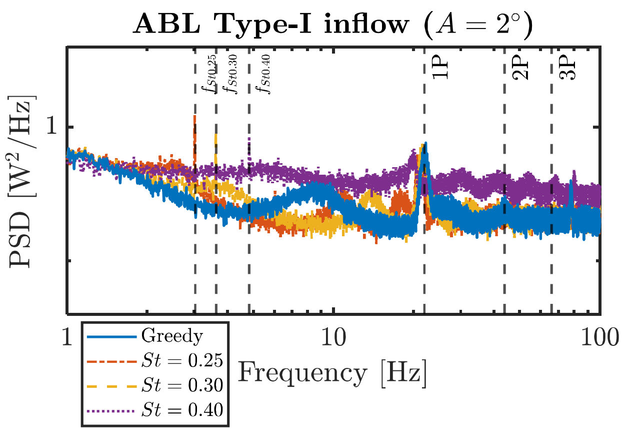

Figure AR02. Illustration of the power spectra of WT1's power signal. Note the increased energy content across a broad range of low frequencies for the DIC case with St = 0.40.

The text has been reformulated as follows:

Under ABL inflow, the power loss at WT1 is generally comparable to that observed under uniform inflow conditions, except for the DIC case with St = 0.40 under ABL Type-I, which exhibits a significantly higher loss of 23.2%. Power spectrum analysis of the torque signal revealed a significant increase in low-frequency energy content compared to other DIC cases, indicating that the loss was driven by large fluctuations in generator torque, which in turn caused significant power fluctuations. This is suspected to have been caused by a bug in the turbine's operating code introducing communication delays in the system after long run-time.

16. Some better explanations of the miniature wind turbines' increased power loss would be helpful. Is there a chance OpenFAST can't capture the unsteady aerodynamics properly? Similarly, was an unsteady aerodynamics (dynamic stall) model applied in OpenFAST?

The increased power losses is a limitation of the model wind turbine, whose power curve is more sensitive to pitch angle variations compared to full-scale turbines (see steady-state C_P comparison between NREL-5MW and MoWiTO 0.6 in the Figure below). Consequently, higher average power losses occur when DIC mode is active. This can be attributed to increased sensitivity and reduced airfoil efficiency in low-*Re* regimes. As mentioned in the original manuscript (L.384 – 386), this behaviour has been also observed in previous wind tunnel experiments with similar model turbines (Frederik et al., 2020; van der Hoek et al., 2022, 2024).

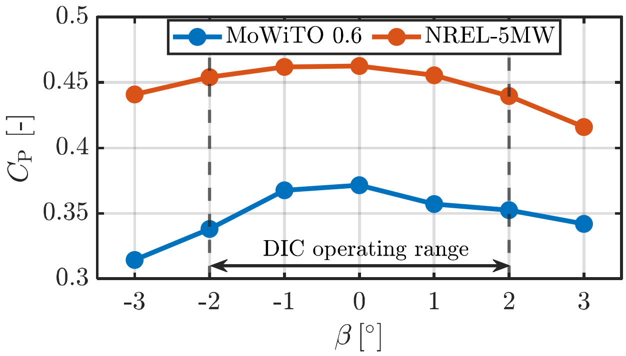

Figure AR03. Illustration of steady-state C_P comparison between NREL-5MW and MoWiTO 0.6

For better clarity, we have reformulated the text in the discussion, as follows:

...the increased power losses are a limitation of the model wind turbine, whose power curve is more sensitive to pitch angle variations, likely due to reduced airfoil efficiency in low-Re regimes. Consequently, higher average power losses occur when DIC mode is active. Such behaviour has been observed in previous wind tunnel studies with comparable model turbines (e.g. Frederik et al., 2020b; van der Hoek et al., 2022, 2024). Nevertheless, the findings highlight the potential wind farm power benefits of DIC implementation in realistic inflow conditions, particularly in low-turbulence environments, which typically exhibit more persistent wakes.

Regarding openFAST simulations, we employed the Beddoes-Leishman unsteady aerodynamic model (see openFAST user documentation), which accounts for dynamic stall effects. However, as noted in L.130, it is worth reminding that DIC is targeted for low-frequency actuation (about 0.017 Hz for the shown simulations at 7 ms^{-1}), whereas dynamic stall is related to rapid changes in the angle of attack. Therefore, despite OpenFAST simulations involving some simplifications, they provide a reasonable indication that power losses in full-scale turbines are likely to be of smaller magnitude. This is further supported by the cited studies (see L.382) on DIC, based on LES simulations using actuator disk or actuator line models.

We have added the following sentence to the Appendix D:

To account for unsteady aerodynamic effects, the Beddoes-Leishman unsteady aerodynamic model is employed.

… despite some simplifications inherent OpenFAST simulations, the results provide reasonable indication that power losses in full-scale turbines are likely smaller than those experienced by the model turbine.

Minor grammatical and formatting comments:

1. Both "setpoint" and "set-point" are used to describe the same concept. Recommend using "setpoint" throughout.

   Thank you for hinting this. We identified one occurrence on L.113 and it has been corrected.

2. **Line 186:** "perpendiculat" should be "perpendicular."

   This typo has been corrected.

3. **Line 279 (and others):** The mathematical function "min" is used as the abbreviation for minutes.

   Thank you for the observation. However, according to the International System of Units (SI) the abbreviation “min” (without a dot) is a non-SI unit accepted to denote minutes. Furthermore, within our context, we believe it is unambiguous that "min" refers to minutes rather than minimisation.

Referee 2

This paper presents numerical experiments of dynamic induction control (DIC) under both laminar uniform and ABL-like inflows. Results are provided for single-turbine cases with different pitching amplitudes and frequencies. The impact of DIC is studied on both the turbine response and the wake. Similar analyses are performed with a second turbine placed downstream of WT1 and operated greedily. The cascading effect of DIC from WT1 wake to WT2 wake is discussed. The potential power gains for a third turbine are eventually presented.

The paper is well-written and the structure is clear, as are the literature review and methodology section. The analyses are precise and interesting elements are discussed, with added contribution to the current state of the literature. Some points could still use clarification or further discussion. Please find them below:

We sincerely thank the referee for their time and effort in thoroughly reviewing our manuscript. Below, we provide detailed responses to each comment and explain how we have addressed them in the revised manuscript.

L.25: "No control strategy is typically implemented to mitigate wake interactions between individual turbines": It is not common practice yet, still some turbine manufacturers have commercial products available for wind farm operators that include wake effects mitigation through wake steering.

Indeed, this is what we meant by "no control strategy is typically implemented". To avoid confusion, we have reformulated the text as follows:

Since technical and economic constraints make wake effects largely unavoidable, advanced wind farm flow control strategies are being developed to mitigate wake losses and ultimately reduce the levelised cost of energy (Meyers et al., 2022). These strategies often involve turbine-level actuation (e.g. yaw, pitch) based on optimal control setpoints to improve inflow conditions for downstream turbines (Houck, 2022). When effectively implemented, this can benefit overall plant performance through increased power production or reduced fatigue loads. Although first commercial solutions are emerging, widespread adoption remains limited, requiring further research and development.

Sec.2 Methodology: A full wake scan takes about 15s, while a DIC actuation period is about 0.27s (St=0.30). Do you believe that scanning through different instants at different locations throughout a periodic phenomenon can be an issue?

Since the scanning period is not a rational multiple of the pitch cycle, each spatial point is captured at a random phase of the actuation. Also, to ensure statistically converged time-averaged results, we measured each vertical plane for approximately 10 minutes, capturing more than 2200 pitch cycles in this particular DIC case. Therefore, we do not see potential issues with the methodology employed.

Sec.3 Results: The "three-turbine set-up" naming is a bit misleading as there is no third turbine. Maybe you can find another formulation that is more representative of the reality.

We have reformulated the text, primarily referring to it as the "virtual three-turbine configuration", and, where necessary, explicitly clarifying which turbines are physical and which are virtual.

L.255: "The ABL case exhibits more pronounced wind speed deficit patches, particularly in the upper region of the velocity field, due to the inflow wind shear." The figure shows the difference in mean wind speed between greedy control and DIC. The effect of shear is also present in the greedy case, so in a linear world, it would cancel out. Does that mean that shear and DIC interact? Can you elaborate?

Thanks for pointing this out. Indeed, since DIC excites instabilities in the shear layer region of the wake and the strongest velocity gradient is located at the upper tip region under ABL inflows, the momentum entrainment from aloft is likely to be higher compared to cases under uniform inflow. To indicate this, we have added the following sentence:

...This can be attributed to the enhanced vertical momentum entrainment triggered by DIC (Brown et al., 2025), which represents a dominant mechanism for energy replenishment in the wake of turbines interacting with boundary layer inflows (Cal et al., 2010).

L.234: "The weighted average wind speed provides a better estimate of the energy available in the wake": Can you substantiate this claim?

Unlike a simple average wind speed across the rotor area, the adopted approach gives a higher weighing to the outer rings (larger area), which better reflects the energy capture of a wind turbine (excluding tip-losses).

To clarify this point, we have reformulated the text as follows:

The u_{REWS} method provides a weighted average wind speed across the rotor swept area, accounting for spatial variations in the velocity field (Wagner et al., 2011). In this study, the rotor area is segmented into five ring segments based on the measured wake cross-sections, as reflected in Eqn. 5

...Since the outer rings cover a larger area, they are weighted more heavily and contribute more to the energy that would be captured by a virtual downstream turbine, neglecting tip-losses.

Fig6: For the uniform inflow and A=1deg, the wind speed gains keep increasing with increasing Strouhal, and, compared to the other inflows, the maximum has not been reached yet. Do you have any experimental data/insight into what would be the optimal St number in the case?

Unfortunately, we do not currently have experimental data to draw conclusions. However, this is an aspect that we intend to investigate in future studies, particularly from a fundamental fluid dynamics perspective.

Connected to this question, we have added the following sentence to the discussion:

...note that the optimal St is influenced not only by the level of induced thrust fluctuations (Sect. 3.1.3) but also by the spatial development of coherent structures (Fig. 8), which is in turn affected by the forcing amplitude and level of inflow turbulence

Section 3.1.2, Discussion on added turbulence: TI is defined through standard deviation sigma, which accounts for any type of fluctuations in the velocity signal, whether they are coherent or random fluctuations (in the sense of triple decomposition). Increase in TI might result from purely random contribution (strictly speaking turbulence), or from coherent structures. The point is: is it really added turbulence in the wake, or is it added fluctuations because of the shedding of vortex rings? Or is it a combination of both? This comment also holds for a sentence at L.355: "enhance turbulent mixing by introducing higher levels of DIC-added local turbulence": is it really turbulent mixing (only) or is there also a coherent structure contribution, as discussed in Munters and Meyers, 2018, and Yilmaz and Meyers, 2018, with the formation of vortex rings? Do you have any hint in the relative importance of coherent and random fluctuations when it comes to increasing TI?

Thank you for pointing this out. A similar comment was raised by Reviewer 1 in numeral 6 and has already been addressed there. We kindly refer the reviewer to that response.

Table2: Under the ABL inflows, C_T increases with DIC, and is higher for higher St numbers. How do you explain this? Is it consistent with previous studies?

To clarify this, we have added the following text:

...experiments under ABL inflow show moderately higher mean C_T even in the baseline greedy case, particularly for the strongly sheared ABL Type-II. This is attributed to the vertical shear, which, unlike uniform inflow, results in a wind centre of pressure (i.e. the point where the resultant wind force acts) located above hub height due to higher momentum in the upper half of the rotor. Since DIC induces periodic thrust oscillations, its interaction with sheared inflow likely causes a shift in the thrust load centre. This leads to an increase in mean C_T with increasing *St*, being most pronounced at *St* = 0.40 due more energetic fluctuations, as indicated by the higher standard deviation

Fig10: This figure shows that, globally, the wind speed gains in WT2's wake are higher than those in WT1's wake. Can you comment on that?

We have added the following text in Sect. 3.2.1:

...the alignment with *St* = 0.30 for both amplitudes is attributed to the higher turbulence levels in WT2's wake, which promote faster wake recovery even without WT1 actuation. Interestingly, the improvement in WT2's wake recovery due to WT1 actuation is similar to, or even exceeds, that of WT1's wake. This is related to the higher turbulence in WT2's wake, as well as to the fact that the energy content of the induced thrust oscillations at WT2 remains comparable to that of the actuated WT1, as described in Sect. 3.2.2. Furthermore, similar trends are observed under ABL inflow, albeit with slightly smaller improvements, as the increased ambient turbulence reduces cascading fluctuations at WT2.

The next response is also connected to this question, see below.

Section 3.2.2 Thrust coefficient of WT2: It could be interesting to show the thrust signal in the frequency domain for WT1 and WT2. This could highlight the peak at f_DIC generated by the actuation of WT1, and how much this peak cascades to WT2 through the wake. That might be more explicit/specific than comparing standard deviations.

Thanks for this observation. We have extended the analysis in Sect. 3.2.2 including a comparison of the power spectra of induced thrust fluctuations for both WT1 and WT2, as follows:

... Fig. 13 compares the power spectra of induced thrust fluctuations ($\phi_{F_T'}$) for both WT1 and WT2, zoomed into the *St* range corresponding to DIC pitch actuation frequencies. Cases under uniform inflow and ABL Type-II are selected to illustrate the cascading behaviour in the spectra for DIC cases with A = 2°. Under uniform inflow conditions, the DIC-induced peaks not only cascade to WT2 but also exhibit energy levels comparable to those observed at the actuated WT1. This is consistent for both amplitude cases, $A \in \{1°, 2°\}$, explaining why the wake recovery improvement of WT2 is similar or even exceeds that of WT1. Also, note that since WT2 operates within WT1's turbulent wake, its thrust fluctuation energy remains higher even when WT1 operates in greedy mode. In contrast, under ABL inflow conditions, the DIC-induced peaks still cascade to WT2 but with lower energy content compared to WT1, due to the dominant role of ambient turbulence, as noted earlier. This also explains the reduced improvement in WT2's wake recovery improvement under ABL conditions.

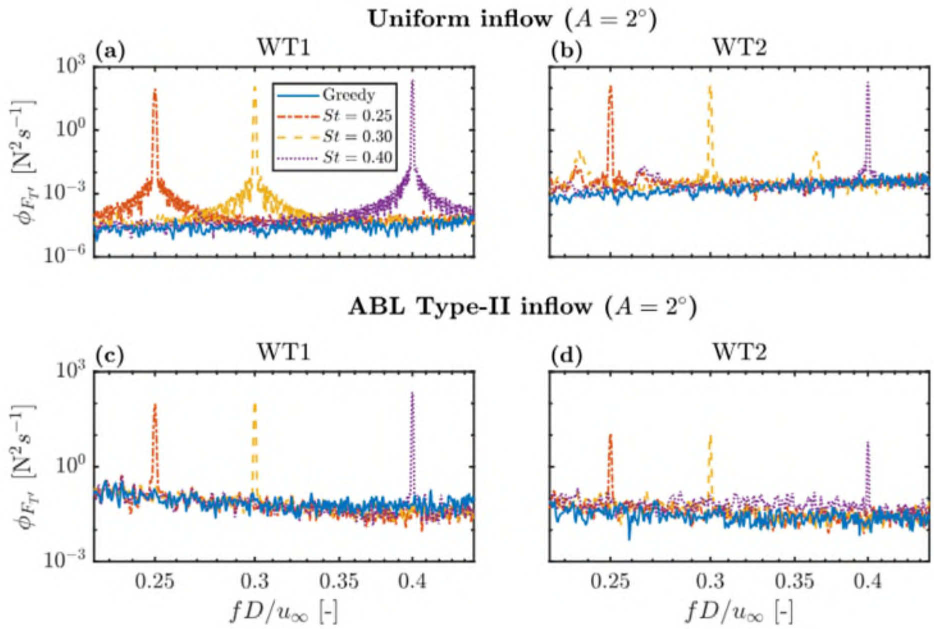

Figure 13. Power spectra of induced thrust fluctuations ($\phi_{F_{T'}}$), zoomed into the *St* range corresponding to DIC pitch actuation frequencies. Only cases under uniform and ABL type-II inflow conditions are displayed to illustrate the cascading effect in response to WT1 operating in greedy or DIC mode, while WT2 remains in greedy mode throughout.

Section 3.3 Wind farm power gains: For the virtual turbine, the assumption is made that its power is computed from u_REWS and C_P = 0.37. It would be valuable to validate this hypothesis with WT2, for which you have real turbine power but can also recompute virtual power from the WT1-only cases. Could you add such a comparison, maybe as an appendix, and validate the virtual turbine assumption?

Thank you for pointing out that. We have added to the Appendix a comparison of the overall power trends using two virtual turbines, while discussing the main observations in Sect. 3.3, as follows:

...it is worth noting that the relative gains based on WT2's power measurements are higher than those estimated from virtual power using WindScanner data (cf. Appendix C1, where WT2's virtual power is computed in the same manner as for virtual WT3). This discrepancy arises from the C_P dependence on *Re*, which reduces aerodynamic efficiency at lower wind speeds. Consequently, the power gain at WT2 reflects both the effective increase in wind speed due to DIC, as well as the increase in C_P The latter is a drawback of wind tunnel testing, resulting in smaller wind farm power gains but without affecting the qualitative trends, as described in Appendix C. In contrast, power estimates at virtual WT3 inherently compensate for the C_P dependence on *Re*, as the virtual power is computed assuming a constant C_P across all cases. This assumption more closely resembles the behaviour of full-scale turbines but leads to higher power estimates for virtual WT3 compared to WT2 measurements. Nevertheless, the overall trends remain consistent regardless of the assumed C_P (cf. Appendix C).

Appendix C: Validation of wind farm power gain trends

To validate the qualitative trends observed in Fig. 14, a virtual three-turbine configuration is considered, where only WT1 is based on power measurements, while WT2 and WT3 are virtual turbines whose power is estimated from u_{REWS} following the method outlined in Sect. 3.3. This approach eliminates the influence of *Re* on aerodynamic efficiency CP of the model turbine, isolating the effect of DIC on wake recovery and downstream performance. Fig. C1 presents the corresponding mean power ratio (Pi/Pref) for individual turbines and the overall wind farm. While the relative magnitude of power gains changes slightly compared to the real–real–virtual configuration used in the main analysis, the qualitative trends remain consistent.

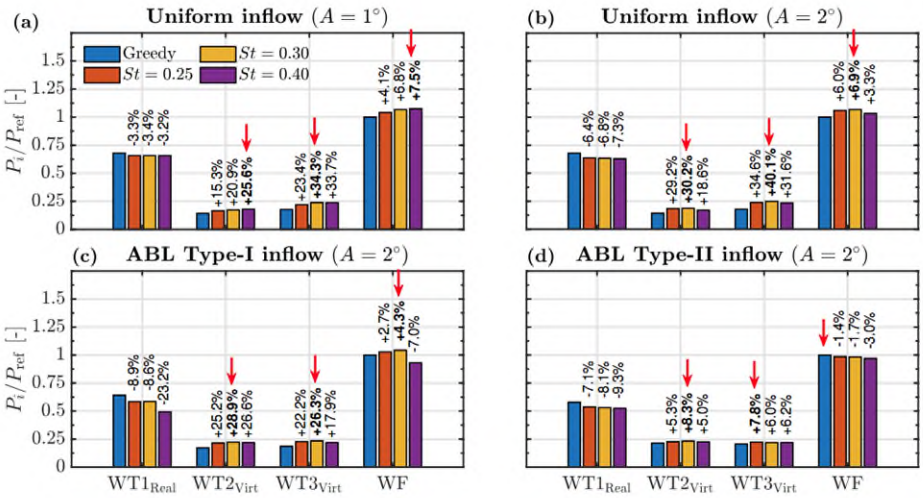

Figure C1. Validation of wind farm power gain trends using a real–virtual–virtual turbine configuration. The power ratio (Pi/Pref) is shown for individual turbines (WT1, WT2, WT3) and wind farm (WF), with WT1 operating in both greedy and DIC modes, while virtual WT2 and virtual WT3 remain in greedy mode. Each subchart corresponds to a different inflow condition. Percentage values indicate the relative change with respect to the baseline greedy case, with Pref representing the wind farm power with all turbines in greedy mode. Red arrows alongside bold text highlight the optimal gains.

Figure 12: It might be worth reminding in the caption of the figure that WT3 is virtual. Can you also comment/explain/add a reference on why the power of WT3 is significantly higher than that of WT2?

We have modified the caption and labels of x-axis to indicate which turbines are real and which are virtual (cf. Appendix. C1 in the previous response and Fig. 14 below).

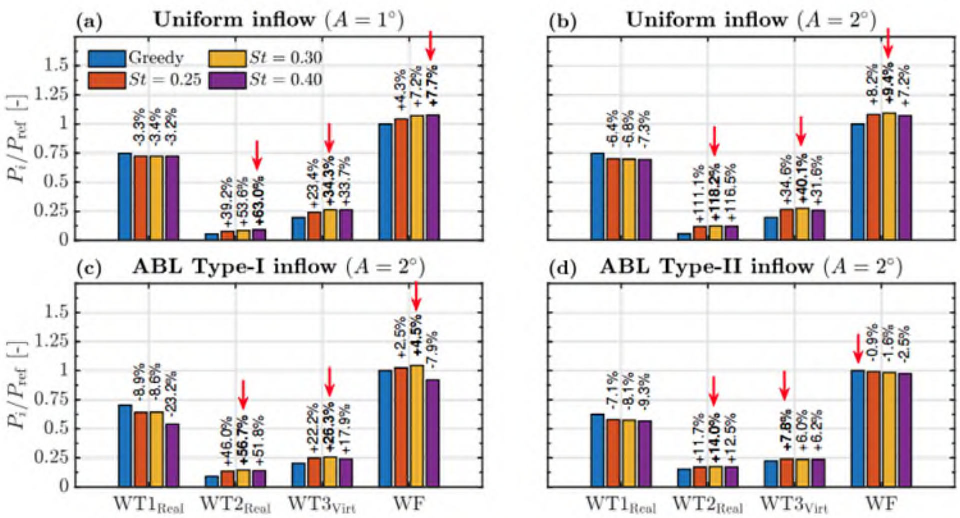

Figure 14. Wind farm power gain using a real-real-virtual turbine configuration. The power ratio (Pi/Pref) is shown for individual turbines (WT1, WT2, WT3) and the overall wind farm (WF), with WT1 operating in both greedy and DIC modes, while WT2 and virtual WT3 remain in greedy mode. Each subchart corresponds to a different inflow condition.

Percentage values indicate the relative change with respect to the baseline greedy case, with Pref representing the wind farm power with all turbines in greedy mode. Red arrows alongside bold text highlight the optimal gains.

Moreover, the higher power at virtual WT3 compared to measured power at WT2 is related to the C_P dependence of the model turbine on Reynolds number. As stated in the previous response:

...power estimates at virtual WT3 inherently compensate for the C_P dependence on *Re*, as the virtual power is computed assuming a constant C_P across all cases. This assumption more closely reflects the behaviour of full-scale turbines but leads to higher power estimates for virtual WT3 compared to WT2 measurements.

L.371: Regarding the asymmetric behavior of the wake re-energization for Type-II inflow, it might be worth considering the work of G. Yalla, K. Brown, L. Cheung, D. Houck et al. Several papers of this group discuss DIC (among other active wake mixing techniques) in realistic offshore wind conditions, i.e. with the presence of shear, turbulence and even veer. Can similarities be found in this asymmetric behavior with such contributions?

Thanks for the suggested work. We have added the following sentences:

...analysis of the wake centre confirmed a reduced lateral deflection across all DIC cases under ABL inflow. This finding aligns with Brown et al., (2025), who similarly observed that DIC reduces wake skew under sheared and veered inflow conditions.

L.404: The discussion about loads comes a bit late. Probably it should already be mentioned from the paragraph before, which recalls that gains are higher for higher pitch amplitudes. It is known, from other active wake mixing techniques (eg. Taschner et al, 2023, doi 10.1088/1742-6596/2505/1/012006), that increasing pitch amplitude directly leads to increased fatigue loads. The trade-off between loads and power is inherent to those techniques.

Thanks for the suggestion. We have reformulated the text in the discussion as follows:

...it can be inferred that the maximum DIC amplitude should be constrained to limit structural loads, as recommended for the helix approach (Taschner et al., 2023). Accordingly, future studies should explore the trade-offs between power benefits and structural load penalties. For instance, Frederik and van Wingerden (2022) reports that DIC primarily affects the tower fore-aft bending moment, without introducing additional risk to the pitch bearing compared to conventional individual pitch control (IPC) for load alleviation. To further investigate load impacts, wind tunnel experiments with aeroelastic model wind turbines capable of meaningful load analysis would be valuable.

Typesetting

L.186: "perpendiculat"

This typo has been corrected

Several expressions that should displayed on a single line are split because that are at the end of a line (Fig1 caption: St=0.30; L.216: $A\in\{1°,2°\}$; L.217: Fig. 5g-1; etc). In the final version of the paper, have a final check and make sure it does not happen using ~ instead of space.

Thank you for pointing this out. The manuscript has been revised accordingly.

L.278: "periodic periodic"

This typo has been corrected

References

Brown, K., Yalla, G., Cheung, L., Frederik, J., Houck, D., deVelder, N., Simley, E., and Fleming, P.: Comparison of wind-farm control strategies under realistic offshore wind conditions: wake quantities of interest, Wind Energy Science Discussions, 2025, 1–39, https://doi.org/10.5194/wes-2024-191, 2025.

Cal, R. B., Lebrón, J., Castillo, L., Kang, H. S., and Meneveau, C.: Experimental study of the horizontally averaged flow structure in a model wind-turbine array boundary layer, Journal of Renewable and Sustainable Energy, 2, 013 106, https://doi.org/10.1063/1.3289735, 2010.

Chamorro, L., Arndt, R., and Sotiropoulos, F.: Reynolds number dependence of turbulence statistics in the wake of wind turbines, Wind Energy, 15, 733–742, https://doi.org/https://doi.org/10.1002/we.501, 2012.

Houck, D. R.: Review of wake management techniques for wind turbines, Wind Energy, 25, 195–220, https://doi.org//10.1002/we.2668, 2022.

Hulsman, P., Wosnik, M., Petrovic, V., Hölling, M., and Kühn, M.: Development of a curled wake of a yawed wind turbine under turbulent and sheared inflow, Wind Energy Sci., 7, 237–257, https://doi.org/10.5194/wes-7-237-2022, 2022b.

Lignarolo, L. E. M., Ragni, D., Scarano, F., Simão Ferreira, C., and van Bussel, G. J. W.: Tip-vortex instability and turbulent mixing in wind-turbine wakes, Journal of Fluid Mechanics, 781, 467–493, https://doi.org/10.1017/jfm.2015.470, 2015.

MATLAB: version 24.1 (R2024a), https://www.mathworks.com, 2024.

Meyers, J., Bottasso, C., Dykes, K., Fleming, P., Gebraad, P., Giebel, G., Göçmen, T., and van Wingerden, J.-W.: Wind farm flow control: prospects and challenges, Wind Energy Sci., 7, 2271–2306, https://doi.org/10.5194/wes-7-2271-2022, 2022

Munters, W. and Meyers, J.: Towards practical dynamic induction control of wind farms: analysis of optimally controlled wind-farm boundary layers and sinusoidal induction control of first-row turbines, Wind Energy Sci., 3, 409–425, https://doi.org/10.5194/wes-3-409-2018, 2018.

Schottler, J., Hölling, A., Peinke, J., and Hölling, M.: Design and implementation of a controllable model wind turbine for experimental studies, J. Phys. Conf. Ser., 753, 072 030, https://doi.org/10.1088/1742-6596/753/7/072030, 2016.

van Dooren, M. F., Campagnolo, F., Sjöholm, M., Angelou, N., Mikkelsen, T., and Kühn, M.: Demonstration and uncertainty analysis of synchronised scanning lidar measurements of 2-D velocity fields in a boundary-layer wind tunnel, Wind Energy Sci., 2, 329–341, https://doi.org/10.5194/wes-2-329-2017, 2017.

van Dooren, M. F., Kidambi Sekar, A. P., Neuhaus, L., Mikkelsen, T., Hölling, M., and Kühn, M.: Modelling the spectral shape of continuous-wave lidar measurements in a turbulent wind tunnel, Atmospheric Measurement Techniques, 15, 1355–1372, https://doi.org/10.5194/amt-15-1355-2022, 2022.

Vermeer, L., Sørensen, J., and Crespo, A.: Wind turbine wake aerodynamics, Progress in Aerospace Sciences, 39, 467–510,560 https://doi.org/https://doi.org/10.1016/S0376-0421(03)00078-2, 2003.

Wang, C., Campagnolo, F., Canet, H., Barreiro, D. J., and Bottasso, C. L.: How realistic are the wakes of scaled wind turbine models?, Wind Energy Science, 6, 961–981, https://doi.org/10.5194/wes-6-961-2021, 2021.

Wagner, R., Courtney, M., Gottschall, J., and Lindelöw-Marsden, P.: Accounting for the speed shear in wind turbine power performance measurement, Wind Energy, 14, 993–1004, https://doi.org/https://doi.org/10.1002/we.509, 2011.

Yılmaz, A. E. and Meyers, J.: Optimal dynamic induction control of a pair of inline wind turbines, Phys. Fluids, 30, 085 106, https://doi.org/10.1063/1.5038600, 2018.